MINISTRY OF EDUCATION AND TRAINING
VIETNAM ACADEMY OF SCIENCE AND TECHNOLOGY

GRADUATE UNIVERSITY OF SCIENCE AND TECHNLOGY

***

TRAN BOI AN

SYNTHESIS OF ANTI−CORROSION COMPOSITES FROM MODIFIED GRAPHENE OXIDE AND POLYANILINE

SUMMARY OF DOCTORAL DISSERTATION ON CHEMISTRY

Major: Organic Chemistry

Code: 9440114

SUPERVISORS

1. Dr. Phan Thanh Thảo
2. Assoc. Prof. Dr. Tô Thị Xuân Hằng

Ho Chi Minh City – 2023

The dissertation is completed at: Graduate University of Science and Technology and Institute of Chemical Technology, Vietnam Academy Science and Technology

Supervisors:
1. Supervisor 1: Dr. Phan Thanh Thao – Institute of Chemical Technology, Vietnam Academy of Science and Technology.
2. Supervisor 2: Assoc. Prof. Dr. To Thi Xuan Hang – Institute of Tropical Technology, Vietnam Academy of Science and Technology.

Referee 1:.....

Referee 2:.....

Referee 3:.....

The dissertation will be examined by Examination Board of Graduate University of Science and Technology, Vietnam Academy of Science and Technology at Institute of Chemical Technology, on …….

The dissertation can be found at:
1. Graduate University of Science and Technology Library.
2. National Library of Vietnam.

PREFACE

1. The neccessary of the study

The most effective anti−corrosion additives are compounds containing chromate (Cr). However, these compounds tend to release Cr (IV) and Cr (VI), which are carcinogenic agents, causing great harm to human health. Many studies have been investigated about the synthesis and application of environmentally friendly corrosion inhibitors, such as inorganic substances (metal oxides and salts, kaolin minerals, hydrotalcite, etc.), organic compounds (several conductive polymers and polymers, plant extracts, sgraphene and graphene derivatives) and hybrid materials ZnO−graphene oxide (ZnO−GO), hydrotalcite−graphene oxide (HT−GO), polyaniline−graphene oxide (PANI−GO) or composites hydrotalcite−polyaniline (HT−PANI), ZnO−polyaniline (ZnO−PANI).

From an overview of domestic and foreign research, we study on "***Synthesis of anti−corrosion composites from modified Graphene oxide and Polyaniline***". Synthesized composites will be applied into PU coating with effective anti−corrosion.

2. Purpose and task of the study

- Investigation of the application of GO in Polyurethane (PU) coating on CT3 steel.
  + Synthesis and characterization of GO.
  + Application of GO in the anti−corrosion coating on CT3 steel.
  + Analysis of protection mechanism of GO in the coating.
- Synthesis and characterizaation of hybrid materials G−HT and G−ZnO, investigation of CT3 steel anti–corrosion.
  + Characterization of hybrid materials G−HT and G−ZnO.
  + Study of anti−corrosion properties of CT3 steel of G−HT and G−ZnO.
  + Study of anti−corrosion mechanism of hybrid materials.
- Synthesis of G−ZnO/PAN and G−HT/PAN and study on anti−corrosion

properties.

+ Synthesis, characterization and study on anti−corrosion of G−HT/PAN composite.

+ Synthesis, characterization and study on anti−corrosion of G−ZnO/PAN composite.

+ Study on anti−corrosion mechanism of G−ZnO/PAN and G−HT/PAN composites.

- Study on CT3 steel protection of PU coating containing G−HT/PAN and G−ZnO/PAN.

+ Preparation anf investigation of steel protection of PU coating containing G−HT/PAN and G−ZnO/PAN.

+ Evaluation of anti−corrosion of coating using EIS.

+ Study on anti−corrosion mechanism of G−HT/PAN and G−ZnO/PAN in PU coating.

3. Scientific hypothesis and new contribution of the dissertation

The dissertion has successfully synthesized and characterized GO using the modified Hummer method. The anti-corrosion performance of the synthesized GO is 77,48%, higher than the previous published results.

Successfully synthesize of hybrid materials G-20HT and G=20ZnO with full characterization of structure, chemical properties. The anti-corrosion performance obtained 96 and 75.78%, respectively.

G−HT/2PAN and G−ZnO/2PAN composites have been successfully synthesized and fully characterized. In NaCl 3,5% medium with 1 g/L of the material, CT3 steel electrode obtained anti−corrosion efficiency of 95,5 and 82,9%, respectively.

Successfully fabricated of PU−(G−HT), PU−(G−HT/1PAN), PU−(G−HT/2PAN), PU−(G−ZnO) and PU−(G−ZnO/2PAN) coating on CT3 steel plates, and characterized the coatings properties. Salt−spray test results show that PU−(G−ZnO/1PAN) film has high protective effect on steel. However,

electrochemical analysis results of PU−(G−HT/2PAN) and PU−(G−ZnO/2PAN) coating have effective protection.

Analysis and determination of CT3 steel anti−corrosion mechanism of GO, G−HT, G−ZnO hybrid materials and G−HT/PAN, G−ZnO/PAN composite as well as CT3 steel protection mechanism of those synthesized material in PU coating.

4. Structure of the dissertation

In addition to the introduction, table of contents,conclusions, annex,list of referrences, the dissertation is divided into 4 chapters with 145 pages, 21 tables, 92 figures and 114 references.

CHAPTER 1: OVERVIEW OF RESEARCH RELATED TO THE DISSERTATION TOPIC

All domestic and foreign references about organic coatings, graphene oxide, graphene oxide−hydrotalcite, graphene oxide−ZnO, polyaniline, composite and applications of above materials in organic coatings have been fully summarized.

CHAPTER 2: EXPERIMENTAL AND METHODLOGY

2.1. Materials and samples

2.1.1. Materials

All chemicals used in this research, such as graphite, $KMnO_4$, H_2SO_4, H_3PO_4, H_2O_2, $Zn(NO_3)_2.6H_2O$, $Al(NO_3)_3.9H_2O$, Na_2CO_3, NaOH, NaCl, HCl, $C_6H_5NH_2$, $(NH_4)_2S_2O_8$, $C_4H_6O_6$ were synthesis grade and purchased from MERCK. For the preparation of PU coatings, polyacrylate as the base and polyisocyanate as the hardener were purchased from Nippon Polyurethane industry (NPU).

2.1.2. Samples

- Series powders of GO, G−HT, G−ZnO, G−HT/PAN and G−ZnO/PAN.
- CT3 steel electrodes.
- CT3 steel plates in size 7x10x0,1 cm which were coated by PU

containing GO, G−HT, G−ZnO, G−HT/PAN and G−ZnO/PAN.

2.2. Synthesis of GO and application in anticorrosion PU coating

2.2.1. Synthesis of GO

5 g of graphite was dispersed in 120 ml of mixture of H_2SO_4:H_3PO_4 (v/v 9:1), 15 g of $KMnO_4$ was added to the mixture and kept at 50 °C for 2 hours. Then, heated to 90 °C for 4 hours. 1−2 mL of H_2O_2 was added to reduce unreacted $KMnO_4$ for 2 hours. GO was exfoliated by 300 KHz ultrasonic for 2 hours, then centrifuged, neutralized and freeze−dried to obtain GO powder.

2.2.2. Preparation of polyurethane coating with GO

GO was dispersed in the solvent by ultra-speed mechanical stirring homogenizer and ultra-sonicated for 1 hour. Mixture of GO and PU was homogenized to obtain GO/PU mixtures, then coated on CT3 steel plates.

2.3. Synthesis of hybrid materials from GO and composites with polyaniline, application in anticorrosion polyurethane coating

2.3.1. Synthesis of G−HT hybrid materials

Co-precipitate the mixture of $Zn(NO_3)_2$ 0,2 M and $Al(NO_3)_3$ 0,1 M into 100 mL of GO solution at pH 9,5-10. Then, the reaction mixture was aged at 80 °C for 24 hours. The co−precipitated product was neutralized by centrifugation, then vacuum dried at 60 °C for 6 hours. A series of G−HT with various m_{HT}/m_{GO} ratios (2/1, 5/1, 10/1, 20/1 and 30/1) was synthesized with over 85% of yield. G-HT was characterized by FT−IR, XRD, SEM and Raman. The anti−corrosion of CT3 steel in NaCl 3,5% medium was studied by weight loss method and electrochemical method.

2.3.2. Preparation of G−ZnO hybrid

GO was dispersed in 50 mL of deionized water then homogenized by ultrasonic bath. $Zn(CH_3COO)_2.2H_2O$ was dissolved in 50 mL of de−ionized water to obtain a solution of $Zn(CH_3COO)_2$ 0,5 M. Solution of $Zn(CH_3COO)_2$was precipitated into GO solution at a flow rate of 3 mL/min, then pH of reaction mixture was adjusted to pH 11 using NaOH 2 M, then

ZnO−GO mixture was obtained. The mixture of ZnO−GO was hydro−thermalized at 110 °C for 16 hours. ZnO−GO precipitate was neutralized with distilled water, vacuum dried at 60 °C for 8 hours.

2.3.3. Synthesis of G−HT/PAN and G−ZnO/PAN composite

G−HT (or G−ZnO) was dispersed in 50 mL of EtOH:H_2O (v/v 50:50), homogenized by sonication for 30 mins. Aniline was dissolved in 50 mL of TA solution, and dropped into G−HT to make aniline−G−HT mixture. APS was dissolved in 50 mL of TA solution to make mixture APS/TA. APS/TA solution was dropped into aniline−G−HT solution, polymerization was kept at 2−4 °C for 8 hours. The products were washed and neutralized, dried at 60 °C, obtained G−ZnO/PAN or G−HT/PAN composites.

2.3.4. Preparation of PU coating containing hybrid materials and composites.

CT3 steel plate samples size 70×100×1 mm were prepared by: (1) Wash oil and grease on the surface with soap; (2) use abrasive paper #400 to clean surface rust; and (3) rinse with distilled water, ethanol and dried.

The synthesized materials were dispersed in the solvent by homogenized for 1 hour. The content of materials in PU was 0,5% wt/wt. Mixture of synthesized materials and PU was homogenized for 30 mins, then coated on CT3 steel plates. The thickness of the dried coating was 15 ± 0,5 μm.

2.4. Analysis methods

2.4.1. Characterization of hybrid materials and composites.

FT−IR spectra was performed on a Fourier transform IR spectrometer, Bruker Tensor 27 (Germany) at the Institute of Chemical Technology. X−ray diffraction (XRD) spectra were analyzed on Bruker Advance D8 instrument (Germany) at Ho Chi Minh City University of Technology. SEM images were observed on a Thermo Scientific scanning electron microscope (USA) at the University of Natural Resources and Environment. Thermo-gravimetric analysis (TGA) of the samples was performed on the DSC−TGA Setaram

system (France) at Ho Chi Minh City University of Education.

Potentio-dynamic polarization curves and coating impedance spectra were analyzed on Biologic VSP equipment at the Institute of Tropical Engineering and at the University of Natural Sciences in Ho Chi Minh City.

2.4.2. Analysis of CT3 steel anti-corrosion efficiency of synthesized materials

2.4.2.1. Weight loss method

The CT3 steel sample has dimensions of Φ 8 × 20 mm, average weight of 8,5 ± 0,25 g, was pretreated and stored in a dehumidifier. Determination of the sample surface area exposed to corrosion (S); weigh the sample before testing m_0. After period of t, sample was taken out and washed off the chemical rust on the surface; rinsed with distilled water and acetone, dried and weight the remaining mass m_s. The mass loss is calculated according to the formula (1) and (2).

$$V = (m_0 - m_s)/S.t \ \ (g/cm^2.day) \qquad (1)$$

$$H = V_s/V_0 \times 100 \qquad (2)$$

In there: H is the anti–corrosion efficiency, %; V_0 and V_s is the mass loss rate of CT3 steel in NaCl 3,5% and synthesized material at the time of sampling, $g/cm^2.day$.

2.4.2.2. Potentio-dynamic polarization method

The potentio-dynamic polarization experiment was performed on Biologic VSP–300 machine using a 3–electrodes system includes: the working electrode is an epoxy–coated steel bar exposed to NaCl medium, the reference electrode is a saturated Ag/AgCl/KCl electrode, and the counter electrode is the Pt electrode. The potentiodynamic polarization curves were measured from the etching potential with a scan rate of 5 mV/s, in the frequency 10^5−10^{-2} Hz.

2.4.3. Coating analysis

2.4.3.1. Salt spray analysis

Salt spray analysis is carried out according to ASTM D610 and ASTM D 714−02 standards. The coatings were tested with salt mist follow to ASTM B−117. The incision on sample is made with a specialized cutting tools.

2.4.3.2. EIS of PU coating containing synthesized materials.

Steel plate samples with/without film coating act as working electrodes. Electrochemical impedance spectroscopy of coating on steel plates were measured on a Biologic VSP machine. Analytical parameters were set in automatic scanning mode in the frequency range 10^5−10^{-2} Hz.

CHAPTER 3. RESULT – DISCUSSION

3.1. Investigation of the application of GO in PU coating on CT3 steel.

3.1.1. Synthesis and characterization on of GO.

3.1.1.1. Characterization of GO.

The FT–IR spectrum (Figure 3.1(a)) of GO has strong peaks at 3401, 1732, 1226 and 1052 cm^{-1} which are assigned for vibrations of carbonyl, epoxy and CO groups. The SEM image shows that GO has a 2D structure, size 1-10 µm, sheet thickness 50–100 nm (Figure 3.2(b)).

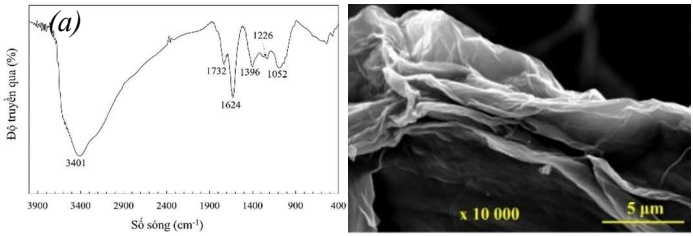

Figure 3.1. FT−IR spectra (a) and SEM image (b) of GO synthesized by modified Hummer method.

3.1.1.2. Study of anti–corrosion of GO on CT3 steel.

The E_{corr} measured on CT3 electrode in blank NaCl medium is -802 $mV_{Ag/AgCl/KCl}$, in NaCl with 1 g/L GO is -740 $mV_{Ag/AgCl/KCl}$ (Figure 3.2). The anti-corrosion efficiency of GO is calculated from Tafel plot is 77,5%. The shift of E_{corr} is 62 mV ((85 mV), so GO is a complex corrosion inhibitor.

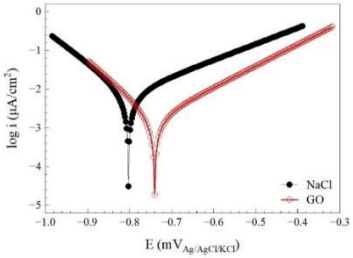

Figure 3.2. The potentiodynamic polarization curves of steel electrode exposed in NaCl 3,5% medium with GO and without GO.

3.1.2. Anticorrosion performnace of PU coating containing GO.

After 21 days immersion, the EIS spectra of PU−(0,1% GO) and PU−(0,3 % GO) coatings have only 1 time constant, while the spectra of blank PU and PU−(0,5 % GO) coatings have 2 time constants (Figure 3.3(a)). Z_{100mHz} of PU−(0,1 % GO) is the highest. PU−(0,5 % GO) and PU coatings have the same Z_{100mHz} and lower than the other two samples (Figure 3.3(b)). This result showed that GO has increased the anti−corrosion effective of PU coatings at concentrations of 0,1% and 0,3%.

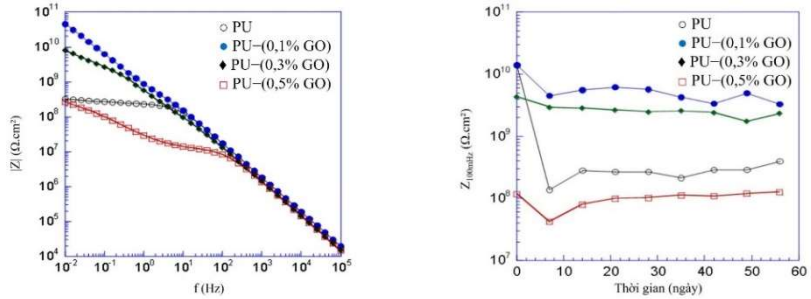

Figure 3.3. Bode diagrams (a) and Z_{100mHz} of PU, PU−(0,1% GO), PU−(0,3% GO) and PU−(0,5% GO) after 21 days immersed in NaCl 3,5% medium.

3.1.3. Anti−corrosion mechanism of GO in PU coating.

The anti–corrosion mechanism of GO has been studied and approved to be synergistic from one or more mechanisms include: barrier mechanism, anode and cathode protection mechanism.

3.2. Synthesis, characterization and study of anti−corrosion behavior of (G−HT) and G−ZnO hybrid materials.

3.2.1. Investigation of the corrosion resistance of G−HT and G−ZnO

hybrid materials by weight loss method.

3.2.1.1. Influence of immersion period in NaCl medium containing hybrid materials.

The anti-corrosion performance of G−HT was 53,4; 54,9; 55,8; 49,3 and 41,4%, respectively (Table 3.1). Similarly, the anti-corrosion performance of G−ZnO was 54,4; 56,4; 57,9; 54,7 and 50,2%. So, G-HT and G-ZnO help to reduce the corrosion rate of CT3 steel in NaCl medium.

Table 3.1: Influence of immersion period of CT3 steel electrode in NaCl 3,5% medium with G−10HT and G−10ZnO for anti−corrosion efficiency.

Period	Blank	G-10HT		G-10ZnO	
(day)	Δm (g)	Δm (g)	H (%)	Δm (g)	H (%)
1	0,03	0,01	54,4	0,01	53,3
2	0,07	0,03	56,4	0,03	54,8
3	0,12	0,05	57,8	0,05	55,5
4	0,17	0,09	53,8	0,08	48,2
5	0,26	0,15	50,1	0,13	41,3

3.2.1.2. Influence of the amount of hybrid materials in NaCl medium.

G−HT and G−ZnO at high concentration caused the decrease of anti−corrosion performance (Table 3.2). The highest anti−corrosion performance was obtained when using 1,0 g/L of material in NaCl medium, which are 61,5 and 66,4% for G−10HT and G−10ZnO, respectively.

Table 3.2: Influence of the amount of G−10HT and G−10ZnO in NaCl medium to the anti−corrosion efficiency (%) in NaCl 3,5%, at 25 °C for 5 days.

Hybrid	Amount of hybrid materials (g/L)				
materials	0,25	0,5	0,75	1,0	1,5
G–10HT	52,5%	55,5%	57,7%	61,4%	60,4%
G–10ZnO	54,0%	57,8%	62,4%	66,4%	64,7%

3.2.1.3. The anti−corrosion efficiency of hybrid materials with various m_{GO}/m_{HT} or m_{GO}/m_{ZnOs}

All the above synthesized G−HT and G−ZnO hybrid materials were dispersed in 1 g/L NaCl medium for 5 days to study the anti−corrosion performance with the results shown in Table 3.3.

Table 3.3: Influence of ratio m_{GO}/m_{HT} or m_{GO}/m_{ZnO} to the anti−corrosion efficiency of synthesized G−HT, 1 g/L at 25 °C.

Anti–corrosion efficiency (%)						
GO	G–2HT	G–5HT	G–10HT	G–20HT	G–30HT	HT
86,9	52,7	56,3	64,2	68,6	61,4	51,0
GO	G–2ZnO	G–5ZnO	G–10ZnO	G–20ZnO	G–30ZnO	ZnO
86,9	58,6	61,9	68,2	69,7	66,4	61,3

3.2.2. Characterization of G−HT and G−ZnO hybrid materials.

3.2.2.1. Study of chemical properties using FT−IR spectra.

In the FT−IR spectra of G−HT, the characteristic peak of GO shifts to the ultraviolet region with a small shift (Figure 3.4). The intensity at 1064 cm^{-1} decreased due to the elongation of alkoxy bonds, the C=O and C−O elongation vibration completely disappeared. The peaks at 429 and 616 cm^{-1} are the vibrations of the metal bonding Zn−O and Al−O.

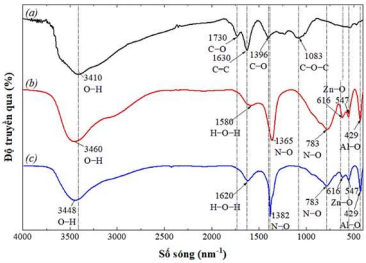

Figure 3.41. FT−IR spectra of GO synthesized using modified Hummer (a), G–20HT (b) and HT (c) synthesized using co–precipitation method.

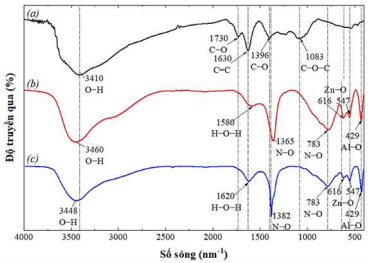

Figure 3.5. FT−IR spectra of GO synthesized using modified Hummer (a), G–20ZnO (b) and ZnO (c) synthesized using precipitation method.

The FT−IR spectra of G−ZnO (Figure 3.5) has all the characteristic vibration of GO. The intensity of the OH and epoxy group was reduced due to the interaction between GO and ZnO, and the wide peak at 481 cm^{-1} was assigned for the vibration of Zn−O.

3.2.2.2. Morphology of hybrid material.

SEM images in Figure 3.18 show that GO has a porous surface and HT flakes were distributed on the GO surface. G−20HT has nanostructures with high pore density. SEM images in Figure 3.6 show that ZnO has a polygonal flake morphology, about 200−300 nm in size.

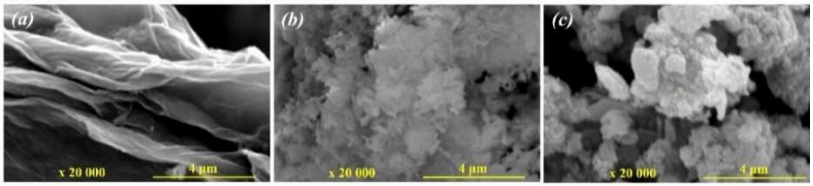

Figure 3.6. SEM images of GO (a), G−20HT (b) and G−20ZnO (c).

3.2.2.3. Crystal structute of G−HT and G−ZnO.

GO has strong XRD diffraction peaks at 10, 11, 17 and 5°, assigned for plane (100) and amorphous materials (Figure 3.7). G−20HT has diffractions coincides with that of HT material at 11, 61 and 62° assigned for plane (003), double layer planes (110) and (113). The results show that HT crystals are attached and grown on GO sheets.

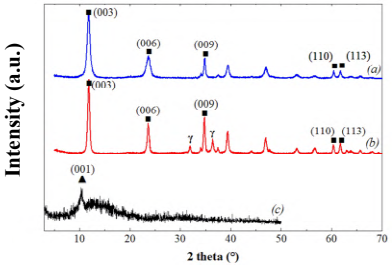

Figure 3.72. XRD patterns of HT (a), synthesized G–20HT (b) and GO (c).

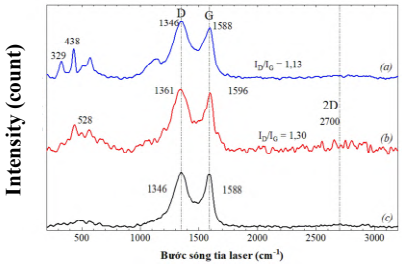

Figure 3.8. Raman patterns of synthesized G–20ZnO (a), G–20HT (b) and GO (c).

The structure of G-ZnO was characterized by XRD at 32, 35, 37, 48, 57, 63, 68 and 69° assigned for (100), (002), (101), (102), (110), (103), (112) and (201) (Figure 3.8). This proved that ZnO particles are attached and grown on GO sheets.

3.2.3. Study of anti−corrosion property of G−HT and G−ZnO

E_{corr} calculated from the potentiodynamic polarization curves of the steel electrode in NaCl medium in the presence of GO, HT and ZnO are −740, −749 and −748 $mV_{Ag/AgCl/KCl}$. Compared to blank sample (E^0_{corr} = −802 $mV_{Ag/AgCl/KCl}$), ΔE_{corr} < 85 mV, so GO, HT and ZnO are complex corrosion inhibitors. E_{corr} of steel in NaCl medium containing G−20HT and G−20ZnO are −496 and −658 $mV_{Ag/AgCl/KCl}$, respectively. ΔE_{corr} >85 mV, so G−20HT

and G−20ZnO play as anode inhibitors.

Tafel extrapolation results show that, in blank medium, i^0_{corr} = 27,7 μA/cm^2. In the presence of GO, HT, G−20HT, ZnO and G−20ZnO, i_{corr} is 6,24; 13,92; 7,77; 14,11 and 6,71 μA/cm^2, respectively. Then, the anti−corrosion performance is 77,48; 71,96 and 75,78%.

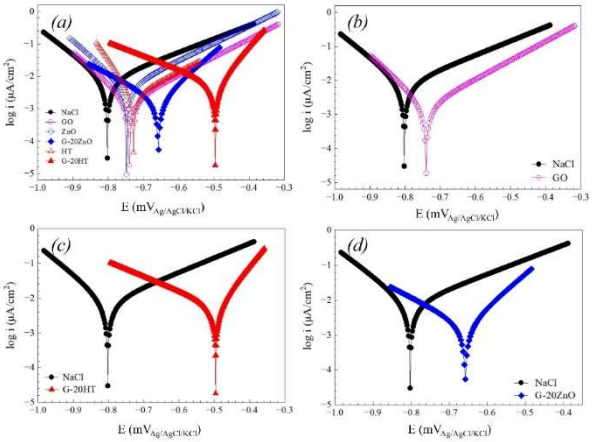

Figure 3.93. Potentiodynamic polarization curves measured on steel electrode exposed in blank NaCl medium and in NaCl 3,5% medium containing GO (b), G–20HT (c) and G–20ZnO (d); 2 hours, 25 °C.

Conclusion: The i_{corr} of steel in NaCl medium containing G−20HT is higher than that of GO, the anti−corrosion efficiency is lower. However E_{corr} shifts to a more positive potential of −496 $mV_{Ag/AgCl/KCl}$.

3.2.4. Analysis of metal protection mechanism of hybrid materials in NaCl medium.

3.2.4.1. Anti−corrosion mechanism of G−HT.

The anti−corrosion mechanism of G–HT hybrid materials is a combination of GO barrier and anion exchange, and trapping Cl^- ions which cause the corrosion reaction occurring in the NaCl medium.

3.2.4.2. Anti−corrosion mechanism of G−ZnO.

After exposing the CT3 steel electrode in NaCl medium containing G–20ZnO, G–20ZnO is physically adsorbed on the electrode surface, forming a physical barrier coating, preventing the contact of corrosive agents to the surface electrode. On the other hand, ZnO has a high hydrophobicity, so the

barrier ability as well as the stability of the G–ZnO film is significantly improved compared to the GO film. As the result, i_{corr} is smaller than when immersed in NaCl medium with GO and G–20HT.

3.3. Synthesis of G–HT/PAN and G–ZnO/PAN and study on corrosion resistance of composites.

3.3.1. Synthesis of G–HT/PAN composite.

3.3.1.1. Influence of m_{G-HT}/m_{PAN} to the structure of G–HT/PAN composite and anti–corrosion efficiency.

FT–IR spectra of G–HT, PAN and G–HT/PAN composite is shown in Figure 3.10. PAN was characterized at 1515 and 1481 cm^{-1} which are elongation strains of benzenoid and quinoid rings. In addition, the bands at 1286, 1116 and 798 cm^{-1} correspond to the in–plane aromatic CH, C−H, and out–of–plane bending vibrations of the benzene ring, respectively. The G−HT/PAN material has the characteristic peaks of PAN shifting to the infrared region at 1578 and 1490 cm^{-1}, showing that HT attached on the surface of PAN, stretching the benzenoid and quinoid ring bonds.

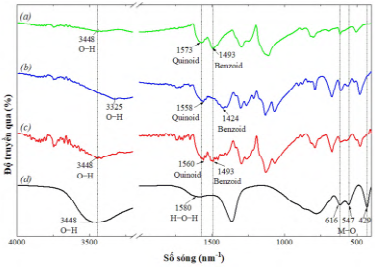

Figure 3.10. FT–IR images of synthesized polyaniline (a), G–HT/1PAN (b), G–HT/2PAN (c) and G–HT (d).

3.3.1.2. Study of anti−corrosion of G−HT/PAN by weight loss method.

As the result in Figure 3.26, the anti−corrosion efficiency of steel in NaCl with G−HT/0,25PAN, G−HT/0,5PAN, G−HT/1PAN and G−HT/2PAN was 67,6; 74,5; 87,5 and 91,4%, respectively. However, G−HT/5PAN obtained the lower anti−corrosion efficiency (80,3%). Compared with GO, the G−HT/1PAN and G−HT/2PAN have higher anti−corrosion efficiency. The results showed that polyaniline increased the

anti−corrosion efficiency of G−HT.

Table 3.4: Anti−corrosion efficiency of composite G−HT/PAN with various mG−HT/mPAN, 1 g/L, study at 25 °C, for 5 days.

Anti-corrosion performance (%)							
GO	G–HT	G–HT/ 0,25PAN	G–HT/ 0,5PAN	G–HT/ 1PAN	G–HT/ 2PAN	G–HT/ 5PAN	PAN
86,9	68,6	67,6	74,5	87,5	91,4	80,3	26,1

3.3.1.3. Characterization and analysis of G−HT/PAN composite.

The structure of G−HT is combined of HT crystals on the surface of GO sheets with diffractions at 2θ of 12, 24, 35, 40, 47, 60 and 62° assigned for (003), (006), (009), (012), (018), (110) and (113), respectively (Figure 3.11). Polyaniline has diffraction at 17, 19 and 25° corresponding to the (011), (020) and (200). The XRD pattern of the G−HT/PAN composite has all the characteristic diffraction of both G−HT and PAN.

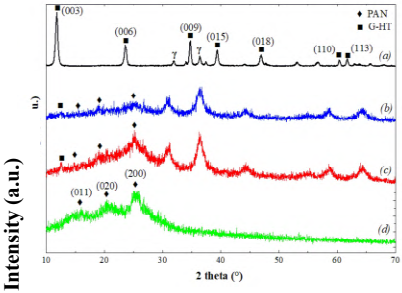

gure 3.11. XRD patterns of ynthesized G–HT (a), G–HT/1PAN (b), G–HT/2PAN (c) and PAN (d).

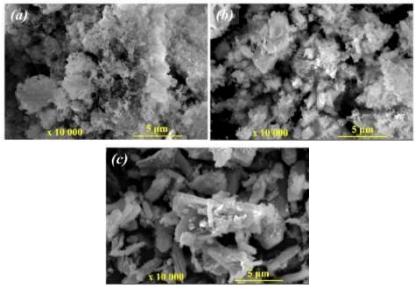

Figure 3.12. SEM images of G–HT (a), G–HT/1PAN (b) and G–HT/2PAN (c) at magnification ×10000.

The morphology of G−HT is the distribution of HT crystals on GO sheets (Figure 3.12). The structure of G−HT/PAN is the combination of PAN needles covered by G−HT flakes.

3.3.1.4. Electrochemical study on CT3 steel corrosion resistance of G−HT/PAN.

The corrosion potential of steel in NaCl medium in the presence of polyaniline, G−HT/1PAN and G−HT/2PAN has a large shift (Figure 3.13), the values are −683, −407 and −382 $mV_{Ag/AgCl/KCl}$, respectively. This shift is

very different towards the anode pole compared to E^0_{corr}, so both polyaniline, G−HT/1PAN and G−HT/2PAN are anode inhibitors.

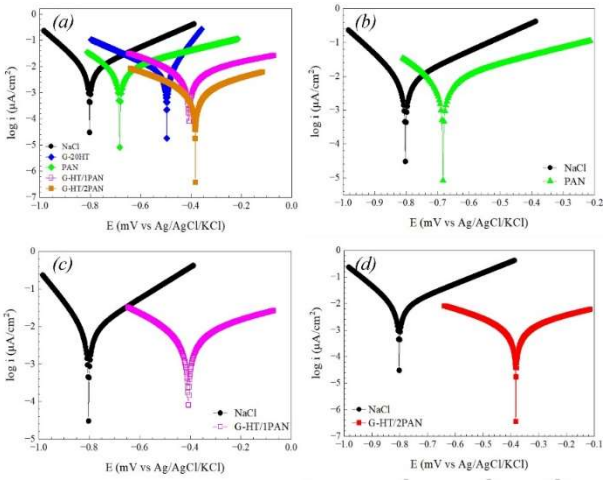

Figure 3.134. Potentiodynamic polarization of CT3 steel electrode immersed in NaCl medium without/with 1 g/L of synthesized polyaniline (b), G–HT/1PAN (c) and G–HT/2PAN (d) for 2 hours at 25 °C.

Tafel extrapolation results show that in the presence of PAN, G−HT/1PAN and G−HT/2PAN, i_{corr} is 6,32, 3,20 and 1,25 μA/cm^2, respectively. It's significantly reduced compared to i^0_{corr} = 27,71 μA/cm^2. The anti−corrosion performance of polyaniline, G−HT/1PAN and G−HT/2PAN are 77,19; 88,45 and 95,49%, respectively.

Conclusion: The results of electrochemical studies shows that G−HT/1PAN and G−HT/2PAN have the same anti−corrosion properties. Therefore, both were used fot fabrication of PU anti-corrosion coating.

3.3.2. Synthesis of G−ZnO/polyaniline composite (G−ZnO/PAN)

3.3.2.1. Characterization of G−ZnO/PAN

The FT−IR spectrum in Figure 3.14 shows that G−ZnO/2PAN has PAN vibration with a shift due to the physical interaction between NH in the PAN chain and G−ZnO. Strong peak at 1550−1600 cm^{-1} increased due to overlap of both C−C vibration of GO and C−N on the quinoid ring of PAN. At the same time, there are characteristic vibration of Zn−O−Zn and Zn−O at 725−750 cm^{-1} and 450−550 cm^{-1}.

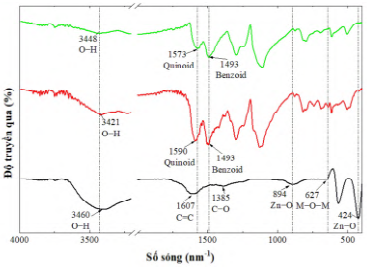

Figure 3.14. FT–IR spectra of synthesized PAN, G–ZnO/2PAN and G–ZnO

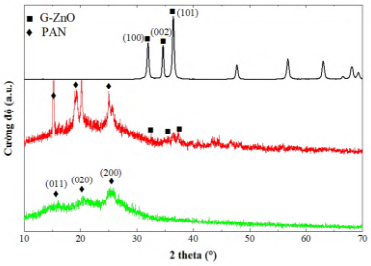

Figure 3.15. XRD patterns of synthesized G−ZnO, G−ZnO/2PAN and PAN.

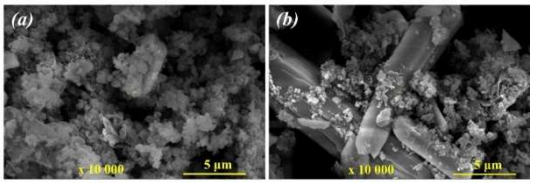

Figure 3.16. SEM images of synthesized G−ZnO (a) and G−ZnO/2PAN (b) at magnification x10000.

G−ZnO/2PAN has sharped peak at 15, 20 and 25 assigned for the (100), (002) and (101) planes, respectively (Figure 3.15). The weak peaks at 37, 44 and 48 correspond to the (102), (110) and (103) planes, respectively. The peaks of G−ZnO/PAN associated to the hexagonal wurtzite structure of ZnO. The morphology of G−ZnO/2PAN was observed through SEM images (Figure 3.16) with G−ZnO covered on the surface of PAN crystal.

3.3.2.2. <u>Electrochemical study on CT3 steel corrosion resistance of G−ZnO/PAN.</u>

The dynamic potential polarization line in Figure 3.37 and the Tafel extrapolation results in Table 3.11 show that in the presence of G−ZnO, G−HT/2PAN and G−ZnO/PAN, the corrosion current density is significantly reduced compared to i_{corr} is 6,71; 1,25 and 4,73 µA/cm^2, respectively. The anti−corrosion efficiency of G−ZnO, G−HT/2PAN and G−ZnO/PAN calculated from i_{corr} are 75,78; 95,49 and 82,93%, respectively.

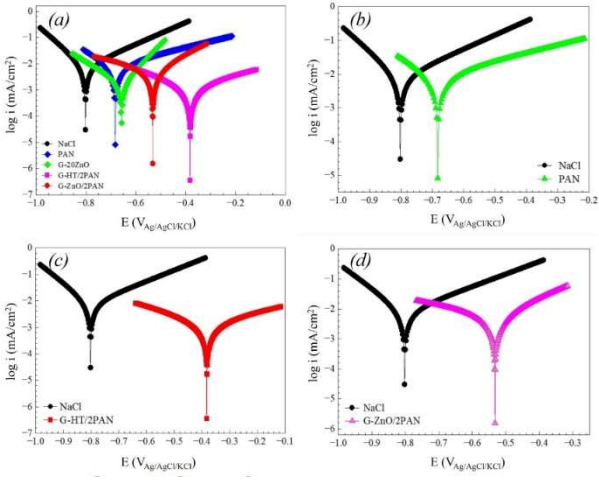

Figure 3.17. Potentiodynamic polarization curves of CT3 steel electrode immersed in NaCl medium without/with synthesized polyaniline (b), G–HT/2PAN (c) and G–ZnO/2PAN (d) for 2 hours at 25 °C.

Conclusion: G−ZnO/2PAN is an anode inhibitor with E_{corr} is −532 $mV_{Ag/AgCl/KCl}$ and i_{corr} is 4,73 μA/cm², anti−corrosion performance is 82,93%.

3.3.3. Anti−corrosion mechanism of G−HT/PAN and G−ZnO/PAN.

Composite was the combination of GO, HT or ZnO and PAN, so that the anti−corrosion mechanism of G–HT/PAN and G–ZnO/PAN composites is a synergistic mechanism from other mechanisms.

3.4. Study of CT3 steel protection of PU coatings with G– HT/PAN and G–ZnO/PAN.

3.4.1. Preparation and study of steel anti-corrosion of PU coating with G–HT/PAN, G–ZnO/PAN by salt spray test.

After 7 days, the PU, PU–(PAN), PU–(GO), PU–(G–HT) and PU–(G–ZnO) samples were all corroded (Table 3.5). Corrosion occurs under coatings. PU–(G–HT/2PAN) and PU–(G–ZnO/2PAN) also had low corrosion. PU–(G–HT/2PAN) has the least danger, the corrosion only developed along the cut, did not endanger the coating. This result is consistent with the results of EIS method analyzed in the following content.

Table 3.5. Optical images of PU coating after 7 days of salt spray test.

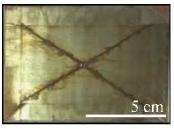	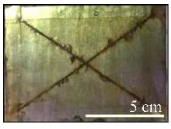		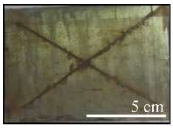
PU	PU−(GO)	PU−(PAN)	PU−(G−HT)
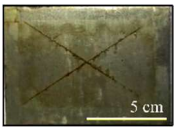		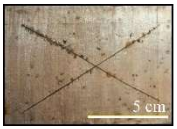	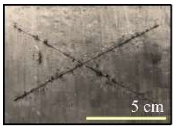
PU−(G−HT/1PAN)	PU−(G−HT/2PAN)	PU−(G−ZnO)	PU−(G−ZnO/2PAN)

3.4.2. EIS study for anti−corrosion property of PU coatings.

3.4.2.1. Anti-corrosion property of GO and G-HT, G-ZnO in polyurethane coating

The Nyquist diagram of PU−(GO) and PU−(G−ZnO) coatings has only 1 arc at high frequencies (Figure 3.18), PU−(GO) and PU−(G−ZnO) have good barrier. The diagram of the PU−(G−HT) coating shows the initial of the second arc in the low frequency region, showing that there's micro-pore in coating structure.

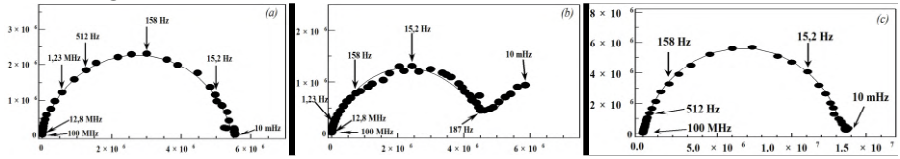

Figure 3.18. Nyquist diagrams of PU–(GO) (a), PU–(G–HT) (b) and PU–(G–ZnO) (c) after 1 day immersed in NaCl 3,5% medium at 25 °C.

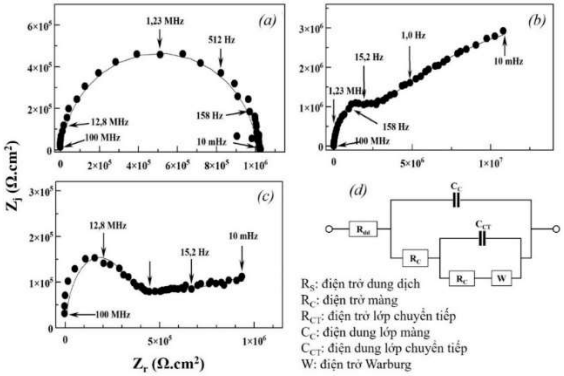

Hình 3.19. Nyquist diagrams of PU–(GO) (a), PU–(G–HT) (b) and PU–(G–ZnO) (c) after 5 days immersed in NaCl 3,5% medium at 25 °C and equivalent electrical circuit used for EIS fitting (d).

After 30 days of immersion, the Nyquist diagrams of all coatings decreased significantly and had 2 arcs (Figure 3.20). The PU−(G−ZnO) coating still shows well barrier due to the reaction between Zn and corrosive elements to form a passivation layer and reduce the corrosion reaction at the contact surface between the coating and the steel substrate.

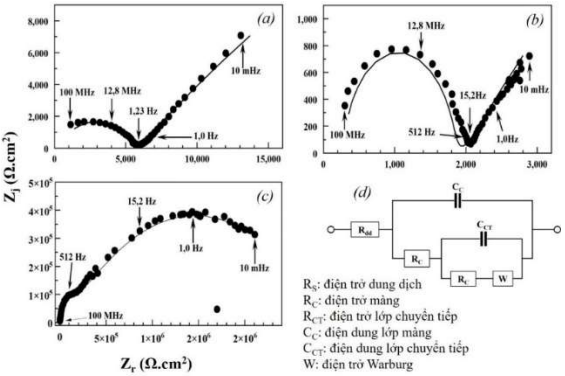

Figure 3.20. Nyquist diagrams of PU−(GO) (a), PU−(G–HT) (b) and PU−(G–ZnO) (c) after 30 days immersed in NaCl 3,5% medium at 25 °C and equivalent electrical circuit used for EIS fitting (d).

The Bode diagrams in Figure 3.21 show that the PU−(GO) coating is the least durable, the Bode curve declines quickly with low Z_{100mHz}. The Z_{100mHz} of the coating is about 10^5 and $1{,}6 \times 10^4$ Ω.cm² after 10 and 30 days. After 30 days, the PU−(G−HT) coating was corroded, the Z_{100mHz} of the coating decreased to $3{,}2 \times 10^3$ Ω.cm². Because G−HT is difficult to disperse in the PU coating and cannot create a uniform coating.

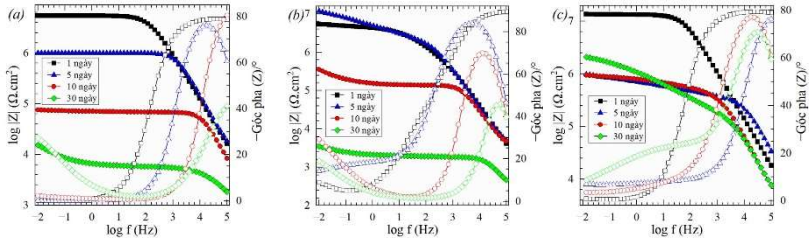

Figure 3.21. Bode diagrams of PU(GO) (a), PU(G–HT) (b) and PU(G–ZnO) (c) coatings immersed in NaCl 3,5% medium at 25 °C.

The PU−(G−ZnO) coating has high impedance, Z_{100mHz} obtained over 10^6 Ω.cm² after 30 days of immersion and had one inflection point in the high frequency region which showed the barrier effect of G−ZnO.

The R_C of the PU−(G−ZnO) is 2,4 × 10^6; 2,1 × 10^6; 1,7 × 10^6 and 0,2 × 10^6 Ω.cm^2 after 1, 5, 10 and 30 days, respectively. The R_C of the PU−(G−HT) coating increased from 3,8 × 10^6 to 4,0 × 10^6 Ω.cm^2 (1 to 5 days), then decreased to 1,9 × 10^3 and 0,4 × 10^3 Ω.cm^2 after 10 and 30 days.

3.4.2.2. Anti-corrosion properties of G−HT/PAN and G−ZnO/PAN composites in PU coating

The Nyquist diagram of the PU−(G−HT/2PAN) coating has only one arc at high frequency, showing that this coating has high barrier. The plots of PU−(G−HT/1PAN) and PU−(G−ZnO/2PAN) coating begin to form the second arc in the low frequency. The reason is G−HT/1PAN and G−ZnO/2PAN dispersed in the PU coating less than G−HT/2PAN. Thus, after only 1 day, electrolyte has diffused into the structure of the coatings.

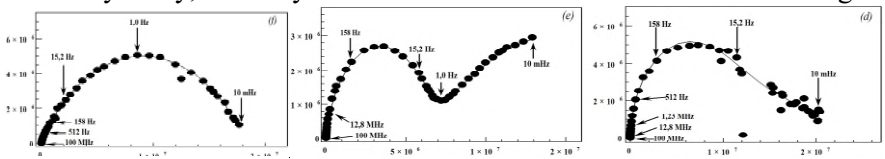

Hình 3.22. Nyquist plots of PU(G–HT/1PAN) (a), PU(G–HT/2PAN) (b) and PU(G–ZnO/2PAN) (c) after 1 day immersed in NaCl 3,5% medium at 25 °C.

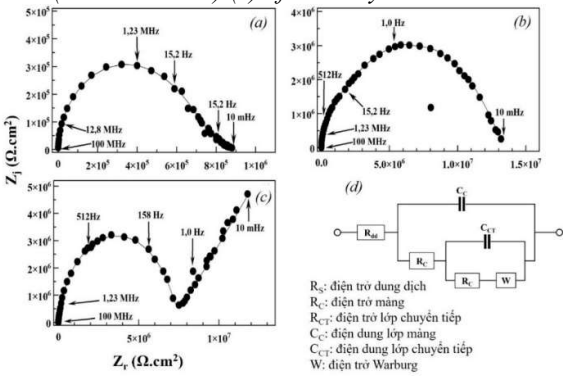

Figure 3.23. Nyquist plots of PU(G–HT/1PAN) (a), PU(G–HT/2PAN) (b) và PU(G–ZnO/2PAN) (c) after 5 days immersed in NaCl 3,5% medium at 25 °C and equivalent circuit (d).

After 5 days, the Nyquist plots of PU−(G−HT/1PAN) and PU−(G−ZnO/2PAN) have two arcs (Figure 3.23). The Nyquist plots of PU−(G−HT/2PAN) coating has only one arc in the high frequency. It proves that electrolyte had diffused through the coating and caused an electrical

reaction. A passive layer was formed and inhibits corrosion. Besides, polyaniline adsorbed the free e^-, reducing the metal dissolution reaction and forming a PAN−LE passive layer with high barrier. After 30 days, the Nyquist plots of all coatings declined and formed two arcs (Figure 3.24). The Nyquist plots of PU−(G−HT/1PAN) and PU−(G−ZnO/2PAN) coatings show lower Z than those of PU−(G−HT/2PAN) coating. That means the PU−(G−HT/2PAN) coating has better barrier than the others.

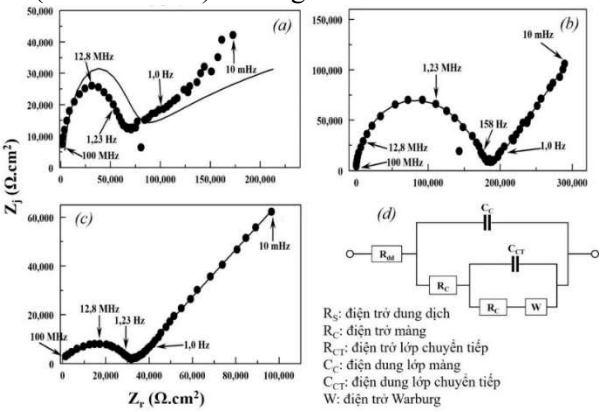

Figure 3.24. Nyquist plots of PU(G–HT/1PAN) (a), PU(G–HT/2PAN) (b) and PU(G–ZnO/2PAN) (c) after 30 immersed in NaCl 3,5% medium at 25 °C and equivalent circuit (d).

The anti−corrosion mechanism of PU−(G−ZnO/2PAN) coating is combined with the anti−corrosion mechanism of G−ZnO and PAN. In NaCl medium, the state of PAN will be changed from EB to LE which has high barrier properties. After 30 days, this Nyquist plots declines significantly.

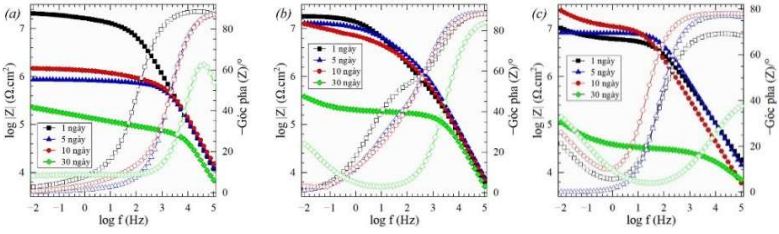

Figure 3.25. Nyquist plots of PU–(G–HT/1PAN) (a), PU–(G–HT/2PAN) (b) and PU–(G–ZnO/2PAN) (c) coating immersed NaCl 3,5% medium at 25 °C.

The Bode plots of PU−(G−HT/1PAN) coating has decreased over time (Figure 3.25). Z_{100mHz} was $2{,}0\times10^7$; $1{,}5\times10^6$ and $2{,}0\times10^5$ Ω.cm^2 after 1, 10

and 30 days. The Bode plots of the PU−(G−HT/2PAN) and PU−(G−ZnO/2PAN) coatings are not too much changed. The $Z_{100\ mHz}$ is above 10^7 Ω.cm^2 after 10 days.

R_C of PU−(G−HT/1PAN) coating decreased from $1,2\times10^7$; $1,1\times10^6$; $8,0\times10^5$ and $4,6\times10^4$ Ω.cm^2 correspond to 1, 5, 10 and 30 days, respectively. For PU(G−HT/2PAN) coating, R_C has decreased from $1,6 \times 10^7$; $8,9 \times 10^6$; $4,6 \times 10^6$ and $0,2 \times 10^6$ Ω.cm^2 after 1, 5, 10 and 30 days, respectively.

3.4.2. Anti−corrosion mechanism of G−HT/PAN and G−ZnO/PAN in PU coating

Both GO and PAN have a protective barrier mechanism that can lengthen the diffusion path of a 3,5% NaCl solution and reduce the rate of electron diffusion to the steel surface. While GO has a large sheet structure that creates a physical barrier, PAN's barrier mechanism is more complex.

In addition, the corrosion protection of G−HT/PAN and G−ZnO/PAN is mainly due to PAN's anode protection mechanism. PU−(G−HT/PAN) and PU−(G−ZnO/PAN) coatings protect steel through both the blocking and blocking capabilities of the composite. PAN will be transformed when receiving e^- from ES to LS state, and the PAN−LS layer when exposed to O on the coating substrate will change from LS to ES state.

Therefore, after the surface passivation layer is formed, electrons are continuously transferred to the external environment, thereby inhibiting the corrosion reaction from occurring. Besides, G−HT and G−HT/PAN can control the corrosion reaction rate due to the ion exchange capacity of both PAN and G−HT. Therefore, the Cl^- from the diffusion of the electrolyte and the e^- generated from the metal surface corrosion reaction can be trapped in the structure of G−HT and especially PAN, from which the redox reaction occurs and causes the anode protection mechanism.

CONCLUSION

This thesis has completed the research objectives with the following main results:

1. The synthesized GO material has a sheet structure with dimensions in the range of 1−10 μm, sheet thickness in the range of 10−100 nm. GO adsorbs on the steel surface which was exposed to NaCl 3,5% medium, anti−corrosion efficiency obtained 77,48%, concentration of 1 g/L. PU coating film with GO has gradually enhance with GO content below 0,5%.

2. The synthesized G−HT hybrid material has a crystalline structure of hydrotalcite tightly attached to GO sheets. Potentiodynamic polarization curves of steel electrode in NaCl medium containing G−20HT has a more positive value, E_{corr} = −496 $mV_{Ag/AgCl/Ks\ \ Cl}$ (E^0_{corr} = −802 $mV_{Ag/AgCl/KCl}$), i_{corr} = 7,77 μA/cm^2, and anti−corrosion performance is 71,96%.

3. G−ZnO has a ZnO crystal structure attached to GO sheets. According to the mass loss method, G−20ZnO has ande anti−corrosion efficiency of 69,70%. Potentiodynamic polarization curves of steel electrode in NaCl medium containing G−20ZnO has E_{corr} = −658 $mV_{Ag/AgCl/KCl}$, i_{corr} = 6,71 μA/cm^2 and anti−corrosion performance is 75,78%.

4. G−HT/PAN has been synthesized and G−HT/2PAN has the highest anti−corrosion performance is 91,4%. G−HT/2PAN acts like an anode inhibitor with electrochemical parameters are E_{corr} = −382 $mV_{Ag/AgCl/KCl}$ and i_{corr} = 1,25 μA/cm^2, the anti−corrosion performance is 95,49%.

5. G−ZnO/2PAN composite was synthesized and acts as an anode inhibitor with electrochemical parameters are E_{corr} = −532 $mV_{Ag/AgCl/KCl}$, i_{corr} = 4,73 μA/cm^2, and anti−corrosion performance is 82,93%.

6. This thesis has manufactured PU−(G−HT), PU−(G−HT/1PAN), PU−(G−HT/2PAN), PU−(G−ZnO) and PU−(G−ZnO/2PAN) coatings and investigate the coatings properties on steel substrates. Salt spray test results show that PU−(G−HT/2PAN) coating has the highest steel anti−corrosion

efficiency. The results of electrochemical analysis of PU−(G−HT/2PAN) coating with Z_{100mHz} are 18,0 × 10^6; 13,0 × 10^6; 12,6 × 10^6 and 3,9 × 10 Ω.cm^2 after 1, 5, 10 and 30 days immersed in NaCl 3,5% medium, respectively. PU−(G−ZnO/2PAN) coating with Z_{100mHz} is 10,2 × 10^6; 8,2 × 10^6; 23,6 × 10^6 to 1,1 × 10^5 Ω.cm^2 after 1, 5, 10 and 30 days immersed in NaCl 3,5% medium, respectively.

LIST OF THE PUBLICATIONS RELATED TO THE DISSERTATION

1.Trần Bôi An, Phạm Minh Vương, Phan Thanh Thảo, Nguyễn Thùy Dương, Trịnh Anh Trúc, Tô Thị Xuân Hằng, ***"Nghiên cứu ảnh hưởng của graphen oxit đến khả năng bảo vệ chống ăn mòn của lớp phủ epoxy"***, Tạp chí Hoá học, ISSN: 0866-7144, 54(6E1), 119, **2016.**

2.Thuy Duong Nguyen, **Boi An Tran**, Ke Oanh Vu, Anh Son Nguyen, Anh Truc Trinh, Gia Vu Pham, Thi Xuan Hang To, Minh Vuong Phan, Thanh Thao Phan, ***Sustainable corrosion inhibitor based on hydrotalcite/graphene oxide nanohybrid for organic coatings***, The 6th Asian Symposium on Advanced Materials: Chemistry, Physics and Biomedicine of Functional and Novel Materials – Proceeding, **2017**.

3.Thuy Duong Nguyen, **Boi An Tran**, Ke Oanh Vu, Anh Son Nguyen, Anh Truc Trinh, Gia Vu Pham, Thi Xuan Hang To, Minh Vuong Phan, Thanh Thao Phan, ***Corrosion protection of carbon steel uisng hydrotalcite/graphene oxide nanohybrid***, Journal of Coating Technology and Research (ISSN 1945- 9645), 16, 585-595, **2019**. Doi:10.1007/s11998-018-0139-3

4.**Boi An Tran**, Thi Xuan Hang To, Thanh Thao Phan, ***Preparation of nanocomposite PANi@GO-HT via dirrectly polymerization from aniline***, The 7th International Workshop on Nanotechnology and Application IWANA 2019.

5.Nguyen Thuy Duong, **Tran Boi An**, Vu Ke Oanh, Pham Gia Vu, Phan Thanh Thao, To Thi Xuan Hang, ***Degradation of polyurethane coating containing graphene oxide under effect of UV radiation***, Vietnam Journal of Chemistry, 58 (3), 333-337, **2020**. Doi: 10.1002/vjch.2019000179.

6.Nguyen Thuy Duong, **Tran Boi An**, Phan Thanh Thao, Vu Ke Oanh, Trinh Anh Truc, Pham Gia Vu, To Thi Xuan Hang, ***Corrosion protection of carbon steel by polyurethane coatings containing graphene oxide***, Vietnam Journal of Chemistry, 58 (1), 108-112, **2020**. Doi:

10.1002/vjch.2013000150.

7. **Boi An Tran**, Huynh Thanh Linh Duong, Thi Xuan Hang To, and Thanh Thao Phan, ***Synthesis and characterization of polyaniline-hydrotalcite-graphene oxide composite and application in polyurethane coating***, RSC Advances, 11, 31572-31582, **2021,** Doi: 10.1039/ D1RA04683G.